Eur. Phys. J. B **46**, 223–230 (2005)
DOI: 10.1140/epjb/e2005-00223-3

THE EUROPEAN PHYSICAL JOURNAL B

Anisotropy and field-dependence of the spin-density-wave dynamics in the quasi one-dimensional conductor $(TMTSF)_2PF_6$

P. Zornoza[1], K. Petukhov[1], M. Dressel[1,a], N. Biskup[2,b], T. Vuletić[2], and S. Tomić[2]

[1] 1. Physikalisches Institut, Universität Stuttgart, Pfaffenwaldring 57, 70550 Stuttgart, Germany
[2] Institut za fiziku, P.O. Box 304, HR-10001 Zagreb, Croatia

Received 3 December 2004 / Received in final form 14 February 2005
Published online 19 July 2005 – © EDP Sciences, Società Italiana di Fisica, Springer-Verlag 2005

Abstract. The anisotropic and non-linear transport properties of the quasi one-dimensional organic conductor $(TMTSF)_2PF_6$ have been studied by dc, radiofrequency, and microwave methods. Microwave experiments along all three axes reveal that collective transport, which is considered to be the fingerprint of the spin-density-wave condensate, also occurs in the perpendicular b' direction. The pinned mode resonance is present in the a and b'-axes response, but not along the least conducting c^* direction. The ac-field threshold, above which the spin-density-wave response is non-linear, strongly decreases as the temperature drops below 4 K. With increasing strength of the microwave electric field and of the radiofrequency signal, the pinned mode and the screened phason loss-peak shift to lower frequencies. In the non-linear regime, in addition to the phason relaxation mode with Arrhenius-like resistive decay, an additional mode with very long and temperature-independent relaxation time appears below 4 K. We attribute the new process to short-wavelength excitations associated with discommensurations of the spin density wave close to commensurability.

PACS. 72.15.Nj Collective modes (e.g., in one-dimensional conductors) – 75.30.Fv Spin-density waves – 74.70.Kn Organic superconductors

1 Introduction

The spin-density-wave (SDW) ground state of one-dimensional conductors attracts considerable attention even after two decades of intensive research. Most experimental studies have been performed on the quasi one-dimensional organic Bechgaard salt di-(tetramethyltetraselenafulvalene)-hexaflourophosphate, denoted as $(TMTSF)_2PF_6$, which soon became the model compound of this phenomenon. Since a large number of results have been accumulated over the years, the SDW state of $(TMTSF)_2PF_6$ can be considered as understood to a fair extent. Nevertheless, there are certain issues which still wait for a clarification [1–3].

At $T_{SDW} = 12$ K, $(TMTSF)_2PF_6$ undergoes a metal-insulator transition below which a thermally activated transport is observed. The insulating SDW ground state is a consequence of the instability of the quasi one-dimensional Fermi surface. In particular NMR experiments reveal that the nesting vector in $(TMTSF)_2PF_6$ is incommensurate: $\boldsymbol{Q} = [0.5a^*, (0.24 \pm 0.03)\, b^*, (-0.06 \pm 0.20)c^*]$ [4].

In the SDW state the optical conductivity develops an absorption edge in the infrared spectral range due to the opening of the single-particle gap at the Fermi energy. While it turned out to be extremely difficult to observe the gap in the direction along the chains because the spectral range is strongly reduced in this range of frequency (so-called clean limit), optical experiments along the perpendicular direction [5] unambiguously proved the development of the SDW gap at $2\Delta/(hc) = 70$ cm^{-1}. The size of the SDW gap detected in dc-limit is much smaller (approximately 30 cm^{-1}), probably due to imperfections inducing in-gap states or due to the dispersion of the energy bands in quasi one-dimensional compounds [6]. A so-called pinned mode resonance is found around 5 GHz; it can be attributed to the collective response of the condensate pinned to lattice imperfections [7]. It contains only a very small fraction of the spectral weight missing after the collapse of the Drude response upon entering the insulating SDW state. At even lower frequencies (in the range of MHz, kHz and even below, depending on temperature) internal deformations and screening by the conduction

[a] e-mail: dressel@pil.physik.uni-stuttgart.de
[b] *Present address*: Instituto de Ciencia de Materiales de Madrid, CSIC, Cantoblanco 28049 Madrid, Spain

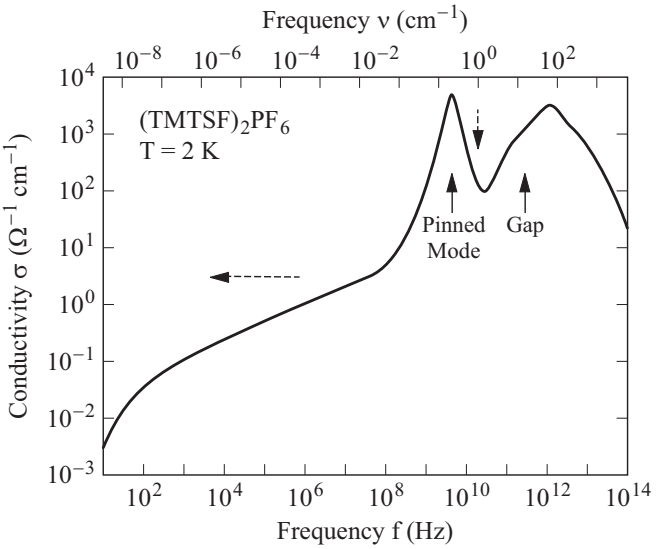

Fig. 1. Sketch of the frequency dependent SDW conductivity composed using various sets of data along the chain axis of $(TMTSF)_2PF_6$. The solid arrows indicate the position of single particle gap and the pinned mode resonance in the microwave frequency range (after [7]). The dashed vertical and horizontal arrows depict the frequency range of the investigations presented in this work.

electrons lead to a broad increase of the conductivity and corresponding broad relaxational behavior. The overall behavior of the optical response is plotted in Figure 1.

A large number of investigations have been dedicated to the non-linear transport of the SDW ground state [7–9]. In very low fields ($E \ll E_T$), as expected for a typical semiconductor, Ohmic behavior is observed along the chains. However in electric fields which exceed a characteristic threshold field E_T, a contribution to the conductivity due to the sliding of the SDW was expected and experimentally found. E_T is typically in the 3–8 mV/cm range in nominally pure specimens, with a factor of two increase of the conductivity in fields which are several times larger than E_T. The existence of both narrow-band noise [10,11] and Shapiro interferences [11] above E_T provide very strong indirect evidence that the nonlinearity observed is associated with a depinning of the SDW, however the large motional narrowing of the proton lineshape seen above E_T [12] is by far the most conclusive proof. As expected for a SDW which is pinned to impurities, the size of E_T has been correlated to the concentration of lattice defects induced by X-ray irradiation [8] as well as to the random disorder introduced by the alloying at the anion sites.

In this communication the issue of the anisotropic and field dependent response of the collective mode is addressed. To our knowledge, the non-linear conduction and the pinned mode resonance – fingerprints of the collective response – have only been investigated along the chain direction. Also not much is known about the radiofrequency and microwave response with increasing amplitude of the driving ac field. Finally, the internal structure of the SDW and the origin of anomalies observed in the spin-lattice relaxation rate, specific heat and magneto-resistance, have not been consistently clarified yet [13–15].

2 Experimental details

Single crystals of the Bechgaard salt $(TMTSF)_2PF_6$ were grown by electrochemical methods as described in reference [16]. After several months we were able to harvest needle-shaped to flake-like single crystals of several millimeters in length (a axis) and a considerable width (b'-direction) up to 2 mm. Here a indicates the stacking direction of TMTSF molecules. Due the triclinic symmetry, b' denotes the projection of the b axis perpendicular to a, and c^* is normal to the ab plane. The crystals were characterized by dc resistivity measurements. Along the a-axis the experiments were performed on needle-shaped samples with a typical dimension of 2 mm × 0.5 mm × 0.1 mm along the a, b', and c^* axes, respectively. The results on the b'-axis conductivity were obtained on a narrow slice cut from a thick crystal perpendicular to the needle axis; the typical dimensions of so-made samples were $a \times b' \times c^* = 0.2$ mm × 1.3 mm × 0.3 mm. Due to our advances in achieving large sample geometry, we were able to measure b'-axis resistivity for the first time with basically no influence of the a and c^* contributions and using standard four-probe technique to eliminate the contact resistance. Also for the c^*-axis transport, we were able to apply four contacts, two on each side of the crystal. The contacts were made by evaporating gold pads on the crystal, then 25 μm gold wires were pasted on each pad with a small amount of silver or carbon paint. The $(TMTSF)_2PF_6$ samples were slowly cooled down to avoid cracks and ensure a thermal equilibrium.

The real and imaginary parts of the conductance, $G(\omega)$ and $B(\omega)$, were measured employing a HP4284A impedance analyzer (f = 20 Hz to 1 MHz) in the two-probe configuration. Three samples with lengths from 0.21 to 0.34 cm and cross-sections in the range of 2.6×10^{-5} to 10^{-4} cm^2 were studied in the temperature range between 1.5 K and 5 K; they all exhibited qualitatively the same behavior. The data were taken by sweeping the frequency at a fixed temperature. Both cooling and warming cycles were conducted and no hysteresis was observed. In order to study the non-linear transport, an ac signal amplitude V_S was applied in the range between 0.07 and 1 of the dc threshold voltage V_T for non-linear conductivity; which at $T = 4.2$ K was in the range from $V_T = 2$ mV to 4 mV. As the smallest ac voltage delivered by the HP4284A is 5 mV, a home-made electronic circuit was utilized to reduce the voltage effective on the sample to the desired level. Dielectric functions were extracted from the conductivity using the relations $\varepsilon'(\omega) = B(\omega)/\omega$ and $\varepsilon''(\omega) = [G(\omega) - G_0]/\omega$. The observed dielectric response can be well fitted by the phenomenological Havriliak-Negami (HN) function widely used to describe relaxation processes in disordered systems

$$\varepsilon(\omega) - \varepsilon_{\mathrm{HF}} = \frac{\Delta\varepsilon}{1 + (i\omega\tau_0)^{1-\alpha}}. \quad (1)$$

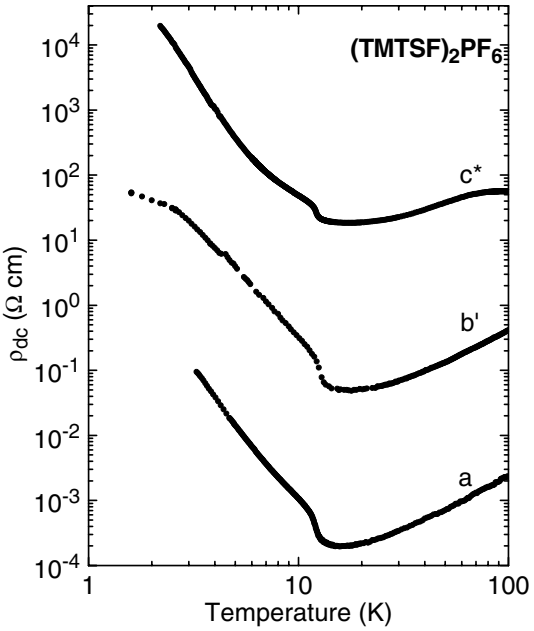

Fig. 2. Temperature dependence of the dc resistivity of $(TMTSF)_2PF_6$ single crystals along the a, b', and c^* crystallographic axes.

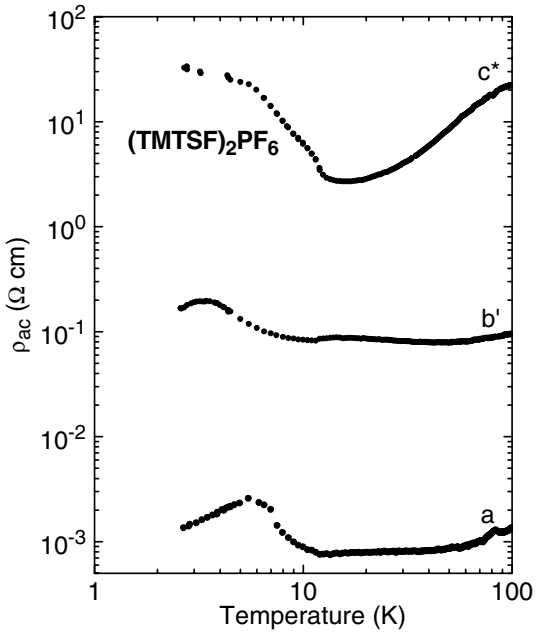

Fig. 3. Temperature dependence of the microwave resistivity of $(TMTSF)_2PF_6$ along the a, b', and c^* crystallographic axes, measured at 33.5 GHz.

Here $\Delta\varepsilon = \varepsilon_0 - \varepsilon_{\rm HF}$ is the relaxation strength, and ε_0 and $\varepsilon_{\rm HF}$ are the static and the high frequency dielectric constant, respectively; τ_0 denotes the mean relaxation time and $1-\alpha$ is the shape parameter which describes the symmetric broadening of the relaxation time distribution function. More details on low-frequency dielectric spectroscopy and the data analysis can be found in reference [17].

In order to measure the microwave conductivity the crystals were placed onto a quartz substrate and positioned in the maximum of the electric field of different cylindrical copper cavities, resonating in the TE_{011} mode at 24, 33.5 GHz and 60 GHz, respectively. Along the a-direction naturally grown needles could be used (typical dimensions of 1 mm × 0.2 mm × 0.2 mm) since this geometry is best for precise microwave measurements. To measure in b' direction, we cut a slice ($a \times b' \times c^* =$ 0.2 mm × 1.2 mm × 0.2 mm) from a thick single crystal. In order to perform microwave experiments along the c^* axis, a crystal was chopped into several pieces (approximately cubes of 0.2 mm corner size) and arranged up to four as a mosaic in such a way that a needle-shaped sample of about $(0.2 \times 0.2 \times 0.8)$ mm^3 was obtained. By recording the center frequency and the halfwidth of the resonance curve as a function of temperature ($1.5\ {\rm K} < T < 300\ {\rm K}$) and comparing them to the corresponding parameters of an empty cavity, the complex electrodynamic properties of the sample, like the conductivity and the dielectric constant, can be determined via cavity perturbation theory; further details on microwave measurements and the data analysis are summarized in [16,18,19]. Using a microwave attenuator in the waveguide line between Gunn diode and the cavity allows us to reduce the power by –18 dB.

3 Results

The temperature dependence of the dc resistivity is displayed in Figure 2, in double logarithmic representation where the SDW transition at $T_{\rm SDW} = 12$ K is clearly seen in all three directions, a, b', and c^*. This is well understood since in this compound the single-particle gap opens over the entire Fermi surface. At lower temperatures the resistivity increases steadily with some exponential temperature dependence $\rho(T) \propto \exp\{\Delta/T\}$ due to excitations across the energy gap ranging from $\Delta \approx 20$ K to 27 K [10]. The results are in excellent agreement with the predictions by the mean-field theory ($\Delta_0 = 1.76\, k_B T_{\rm SDW} = 21$ K) and previous findings [3].

The results obtained for the microwave response at 33.5 GHz are plotted in Figure 3. The SDW transition at $T_{\rm SDW} = 12$ K is again present in all orientations. In contrast to the dc response, however, for lowering the temperature the microwave resistivity increases monotonously below $T_{\rm SDW}$ only in the c^* direction. For the electric field parallel to the chains and along the b' direction, the behavior is more complicated; the resistivity saturates below approximately 4 K and in some cases even a maximum in $\rho_{ac}(T)$ is reached around $T \approx 4$ K below which the resistivity decreases again.

3.1 Anisotropic response of the SDW condensate

In the temperature range slightly below $T_{\rm SDW}$, but still for $T > 4$ K, $\rho(T)$ may be described by an activated behavior, as depicted in Figure 4 [21]. The activation energy along the a and b' axes ($\Delta \approx 5.9$ K and 6.0 K, respectively) is much smaller compared to the dc behavior, while for the c^*

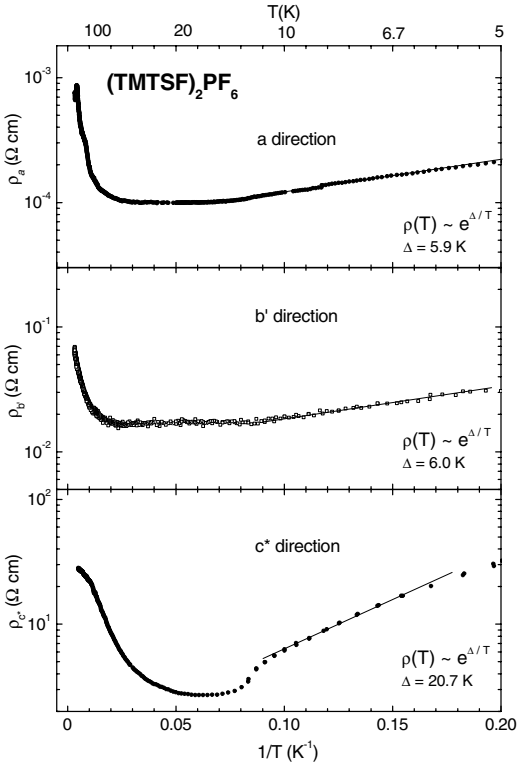

Fig. 4. Arrhenius plot of the microwave resistivity of $(TMTSF)_2PF_6$ along the a, b' and c^* directions measured at 33.5 GHz.

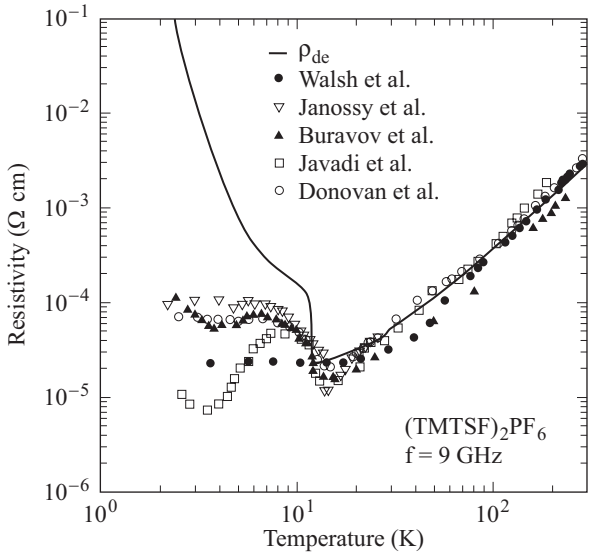

Fig. 5. Comparison of the temperature dependent microwave resistivity of $(TMTSF)_2PF_6$ along the a axis reported by different groups. Data taken from Walsh et al. [22], Janossy et al. [23], Buravov et al. [24], Javadi et al. [25], and Donovan et al. [7]. For better comparison the data have been normalized to the 100 K dc value.

orientation the results at microwave frequencies perfectly agree with the dc profile: $\Delta = 20.7$ K.

3.2 Field dependent response of the SDW condensate

Even more surprising is the decreasing resistivity for temperatures $T < 4$ K. Although the actual shape, its temperature dependence and magnitude varies from sample to sample, the non-monotonous temperature dependence and overall behavior is robust. Up to six samples of different batches have been studied for each orientation leading to very similar findings. In fact, this puzzling behavior was occasionally reported by different groups [7,22–25] over the years, unfortunately without providing any meaningful explanation. In Figure 5 the results for measurements conducted at approximately 9 GHz are compiled.

Donovan et al. [7] also investigated the microwave response at different frequencies from 3 to 150 GHz, and found that the deviations from the dc transport become less when going to higher-frequency resonance cavities [26]. Note, however, that the output power of the microwave source and thus the electric field strength inside the cavity strongly decreases with higher frequencies. It is also interesting to note, that the effect is less pronounced in those cases where the sample is located in the maximum of the magnetic field compared to measurements in the electric field maximum of the cavities. The present work tries to disentangle the influence of frequency and field strength.

In order to further explore the non-monotonous behavior of $\rho_{ac}(T)$, we performed the cavity perturbation experiments along the a and b' orientation using different microwave power, i.e. as a function of the electric field strength inside the cavity. The output power of the Gunn oscillator was attenuated from 0 to –18 dB. The power $P_{\rm input}$ coupled into the cavity varies from 120 μW to 2.5 μW, resulting in a reduction of the average electric field $E \propto \sqrt{P_{\rm input}}$ from 54 mV/cm to 8 mV/cm; in the antinode the field strength is larger by a factor of two. Note, however, that the absolute values only give a rough estime (within a factor of 5) due to uncertainties in the coupling to the cavity and losses in the waveguides. While Walsh et al. [22] estimate 1 mV/cm in their cavity, Buravov et al. [24] give 30 mV/cm for their 9 GHz measurement. The latter group observed no change of the response when the electric field is reduced by a factor of 4. In Figure 6 the microwave resistivity is plotted as a function of inverse temperature for different values of the microwave power [21]. Reducing the power leads to a sharper increase below $T_{\rm SDW}$ and the maximum in $\rho(T)$ shifts to higher temperature; the drop of the low-temperature resistivity becomes even more pronounced. This behavior is robust and was confirmed for different samples. Although this sort of field dependence is more or less observed for both orientations, along the a and b' directions, due to the higher resistivity, the experiments are more precise for $E \parallel b'$ and can cover a larger range of applied microwave power.

In Figure 7 the power dependence of the resistivity ρ_a and $\rho_{b'}$ is plotted for a fixed temperature $T = 2.5$ K. In both cases a linear dependence on the input power is

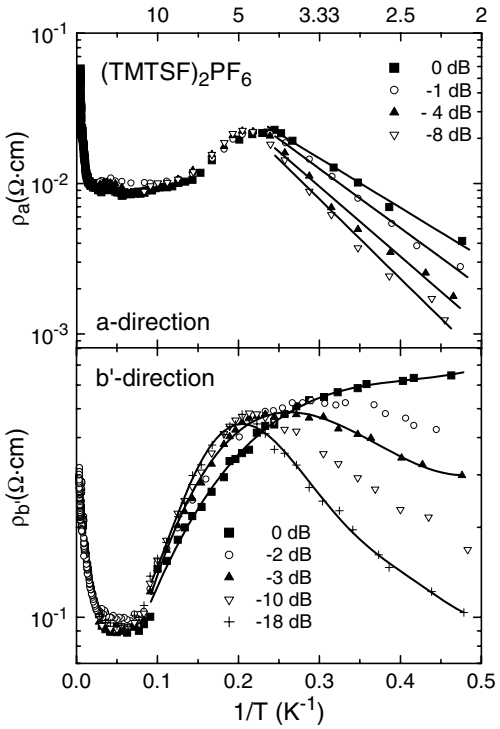

Fig. 6. Resistivity of $(TMTSF)_2PF_6$ as a function of inverse temperature (Arrhenius representation) for different attenuation of the applied microwave power as indicated, leading to different strength of the microwave electric field inside the cavity. The experiments are performed at 33.5 GHz with the electric field oriented (a) parallel and (b) perpendicular to the chain direction.

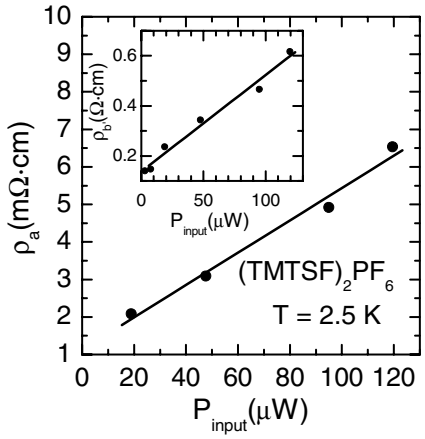

Fig. 7. Resistivity of $(TMTSF)_2PF_6$ along the chain direction of $(TMTSF)_2PF_6$ measured at $T = 2.5$ K versus power put into the 33 GHz cavity. The inset shows the power dependence in the b' direction.

found with an increase by a factor of 4 in resistivity when the input power changes from 3 μW above 120 μW.

For a better understanding of the relation between SDW response and ac signal amplitude, frequency dependent conductivity measurements along the a-direction were performed in the radio frequency range (20 Hz to 1 MHz) at different temperatures by changing the amplitude of the ac voltage V_S. A deviation from the linear behavior is observed if the applied ac signal amplitude V_S increases above a certain threshold voltage $V_S^{\max}$ which also strongly depends on temperature. In Figure 8 the temperature dependence of V_S, normalized to the dc threshold voltage V_T, is shown. The values of V_T at 4.2 K correspond to the threshold field of approximately 6 mV/cm to 10 mV/cm for the single crystals measured, which are typical values reported in this material [8]. For these samples no appreciable temperature change was detected in accord with previous results [8]. However, we should point out that different temperature-dependent behaviors of E_T were also reported [27]. Subtle variations of the disorder level in nominally pure samples were suggested to be responsible for these discrepancies, however no consistent understanding has been achieved yet.

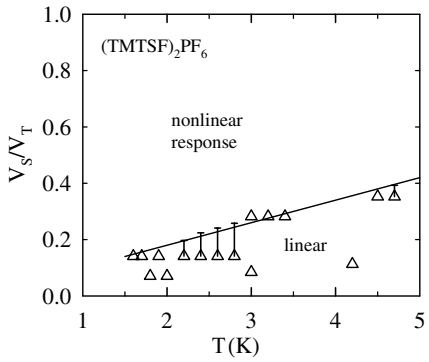

Fig. 8. ac-signal amplitude V_S normalized to the dc threshold V_T, vs. temperature. For $V_S > V_S^{\max}$, where $V_S^{\max}$ is denoted by the full line, the sample response starts to deviate from the linear behavior. The triangles denote values V_S/V_T for which the linear response was observed.

The upper and lower panels of Figure 9 show the real and imaginary parts of the dielectric constant as a function of frequency measured at $T = 3$ K for low ($V_S < V_S^{\max}$) and high ($V_S > V_S^{\max}$) ac amplitudes, respectively. While the observed dielectric response for very low ac fields was successfully fitted by a single HN mode of equation (1), similar attempts (dashed lines) to fit the data measured for higher fields failed. Consequently we tried to describe the data by the sum of two HN modes and achieved an excellent fit. The full lines in Figure 9 correspond to the calculated fits to one (upper panel), or sum of the two HN functions (lower panel). A striking new result is that in addition to the already reported mode with $\Delta\varepsilon$ of the order of 10^9, there is a mode centered at lower frequencies with one order of magnitude larger strength $\Delta\varepsilon \approx 10^{10}$ which occurs only at temperatures lower than 4 K.

The dielectric strength $\Delta\varepsilon$ and the mean relaxation time τ_0 of these two modes are plotted in Figure 10 as a function of inverse temperature. The parameter $1 - \alpha$, which describes the symmetric broadening of the relaxation time distribution function, is temperatures independent and similar for both modes: $1 - \alpha = 0.85$. Triangles (open and full symbols for low and high ac fields, respectively) stand for the mode already reported previously,

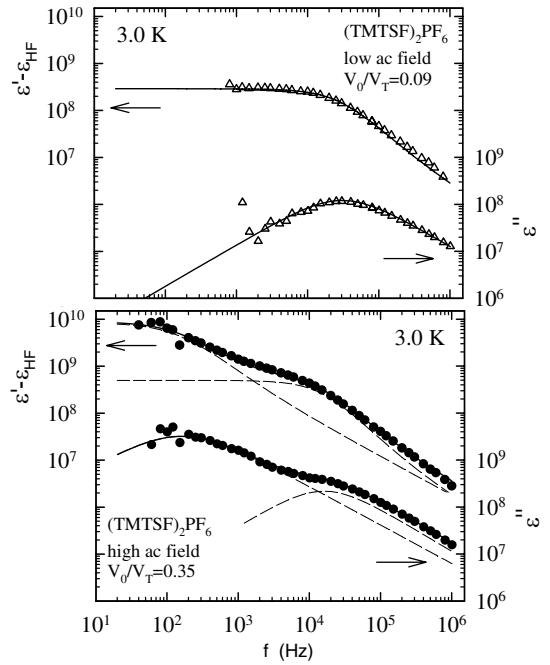

Fig. 9. Double logarithmic plot of the frequency dependence of the real and imaginary parts of the dielectric function at $T = 3$ K for low (upper panel) and high (lower panel) ac amplitudes. The full lines are fits to the HN forms; the dashed lines represent the single HN form.

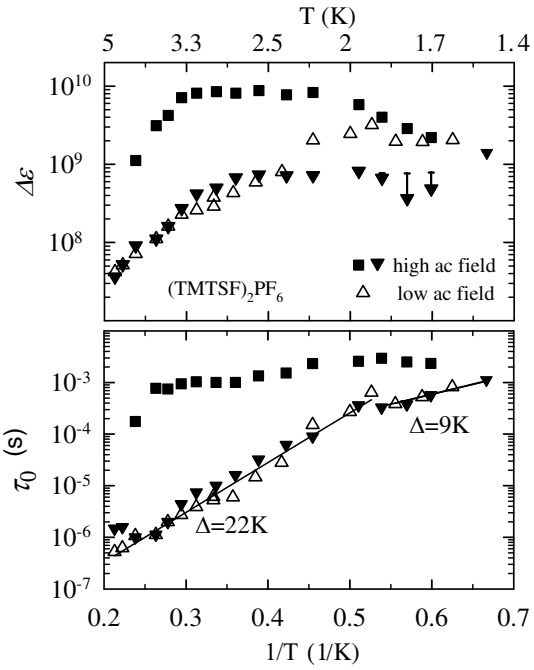

Fig. 10. Relaxation strength (upper panel) and mean relaxation time (lower panel) vs. inverse temperature. Triangles and squares for HF and the LF relaxation mode, respectively. Open and full symbols for low and high ac fields, respectively.

and full squares (for high ac fields) stand for the new mode observed in this study for the first time. We will refer to these modes as high frequency (HF) and low frequency (LF) mode, respectively.

There are two effects induced by ac amplitudes V_S larger than $V_S^{\max}$ (see Fig. 8): First, the number of low-frequency relaxations increases, which effectively shifts the SDW loss peak to lower frequencies. Such an effect was previously observed for charge density waves and attributed to long-time relaxations from metastable states far from equilibrium in which the charge density wave is brought by large ac-signal amplitudes [8]. Second, an additional mode appears below 4 K, with much longer and temperature-independent mean relaxation time $\tau_0 \approx 10^{-3}$ s. At temperatures lower than 2 K, the LF mode converges to the HF one, so that below 1.7 K only one mode can be resolved (Fig. 10).

4 Discussion

4.1 Anisotropy of the collective SDW response

The significantly reduced values of the activation energy found in the microwave resistivity right below the SDW transition at $T_{\rm SDW}$ for the a and b' directions compared to dc data infer a strong frequency dependent response which is associated with the collective mode contribution to the electrical transport. It can be seen in both orientations, a and b', but not in the c^* direction.

It is worthwhile to consider the entire spectrum of the SDW response as suggested by G. Grüner and collaborators [3,7,19] (Fig. 1) Based on an extensive microwave study along the chain direction, it was proposed [7] that due to impurity pinning the collective SDW response in $(TMTSF)_2PF_6$ is located around 5 GHz. At first glance, the conductivity below the energy gap decreases exponentially with decreasing temperature, except in the range of the pinned mode. As can be seen from Figure 1, the present microwave experiments are performed in the range where the collective mode is still very pronounced, i.e. on the high-frequency shoulder of the pinned mode resonance. Hence the temperature dependent microwave conductivity is caused by two opposing effects: (i) the exponential freeze-out of the background conductivity caused by the uncondensed conduction electrons, and (ii) the build-up of the collective contribution. It was suggested that this mode does not gain much spectral weight as the temperature decreases, but the width and center frequency changes slightly [7]. As discussed in reference [20] the presence of the enhanced microwave conductivity not only along the chains, but also perpendicular to them implies that the pinned mode resonance is present in the b' direction in a very similar manner compared to the a axis. Hence the sliding density wave has to be considered a two-dimensional phenomenon.

These results can be explained by looking at the actual Fermi surface of $(TMTSF)_2PF_6$ which is not strictly one-dimensional but shows a warping in the direction of k_b (and much less in k_c). From NMR experiments [4] it is known that the SDW corresponds to a wavevector

$\mathbf{Q} = [0.5a^*, 0.24b^*, -0.06c^*]$; which is slightly incommensurate with the underlying lattice along the b^*. Most important in this context, there is a four-fold periodicity in the real space not only along the best conductivity a-axis, but also perpendicular to it, i.e. along the b-axis. The tilt of the nesting vector is responsible for the similar collective SDW response found in the microwave experiments along the a and b' directions.

4.2 Field dependence of the collective SDW response

It is more difficult to explain the anomalous microwave response at even lower temperatures ($T < 4$ K). The pinned SDW mode shifts to higher frequencies as the temperature decreases [7] and this can even lead to a decrease of the resistivity at certain frequencies. The non-monotonic behavior is therefore due to the decreasing single particle contribution while at the same time the pinned mode shifts into the relevant frequency window. Increasing the electric field makes this effect smaller since the pinned mode might remain at lower frequencies. The spectral weight is likely to be conserved. The effect can be readily understood in the simple picture of the washboard potential [3] which becomes anharmonic for larger driving force. In the real material, the impurity pinning centers are randomly distributed implying a distribution of metastable states around the equilibrium. This is reflected in the inhomogenously broadened resonances of the pinned mode, and in the broad loss peak in the radio-frequency range. Large ac electric fields, but still smaller than dc threshold for sliding, can drive the SDW into metastable states with longer relaxation times far from equilibrium configuration. As a result, the screened loss peak of the SDW shifts to lower frequencies. Similar effect can happen to the pinned SDW mode in the case of high frequencies. In particular the ac threshold field for non-linear response is strongly temperature dependent; hence at low enough temperatures the electric field applied to the sample inside the cavity could be high enough to exceed E_T for ac fields. The sample dependence is caused by variations of the impurity concentration which act as pinning centers.

The deviation from the activated response in the microwave range sets in pretty abruptly below $T = 4$ K, where in the radio-frequency range the LF mode appears. The relaxation of this LF mode is governed by very low energy barriers of the order of a few Kelvin in contrast to the HF process whose relaxation is governed by the single-particle gap as it is the case for the dc conductivity. While the over-all behavior of the HF mode can be ascribed to the screened phason excitations, the spatial variations of the SDW, which is active in the LF process, should be restricted to rather narrow localized regions, so that the associated excitations (like solitons or domain walls) cannot contribute substantially to the dc conductivity. In addition, the almost temperature-independent mean relaxation time indicates that the free-carrier screening, whose influence remains to be visible in the HF process is insignificant for the LF process. This also implies that the relaxation entities in the LF process are much more localized in comparison to the entities responsible for the HT process [17,29]. Furthermore, the temperature behavior of the dielectric strength associated with the LF process indicates that the mode gains the full spectral weight at about $T = 3.3$ K, and starts to diminish again below 2 K merging eventually into the HF mode below about 1.6 K.

The observed dielectric and microwave responses seem to be manifestations of the same phenomenon: i.e. the transition from an incommensurate to a commensurate spin density wave, as suggested by NMR experiments [12,13]. However, this transition is not a simple one, since the NMR lineshape is qualitatively the same above and below the transition and the peak-to-peak width of the absorption derivative is continuous across the transition. From the relaxation rate $1/T_1$ of ^1H-NMR Takahashi et al. [13] constructed a phase diagram with three SDW subphases separated at 3.5 K and 1.8 K at ambient pressure. Note that these temperatures of the second SDW subphase define the region for which the LF mode is dominant when the ac-amplitude V_S exceeds $V_S^{max} = 0.1 - 0.3\,V_T$. We suggest that discommensurations, separating randomly distributed domains of $N = 4$ SDW, might be the most plausible candidate for the relaxation entity of the LF mode. Keeping in mind that the SDW subphase is not a simple commensurate SDW phase, the observation of a random domain structure, as indicated by the value of the relaxation time distribution function $1 - \alpha < 1$, might not be surprising. However, we note that a regular distribution of domain walls (kinks or discommensurations) has been theoretically predicted for the case of complete commensurate-incommensurate lock-in transition [30]. We would like to point out that a similar broad mode, associated with domain walls, has been already obtained in commensurate density waves established in the κ-(BEDT-TTF)$_2$Cu[N(CN)$_2$]Cl and in the deuterated copper-DCNQI materials [31]. In the former, the domain pattern is generated by the canted antiferromagnetic order, while in the latter, it comes from the coexistence of the $N = 3$ density-wave phase and metallic phase in the broad hysteretic region. Only at temperatures well below the transition temperature, a regular domain structure was progressively restored indicating that the long-range commensurate order was fully established. In contrast to that, the LF mode associated with the domain pattern in the SDW sub-phase of (TMTSF)$_2$PF$_6$ seems to disappear below 1.7 K.

5 Conclusions

The dc and microwave conductivity in the SDW state of (TMTSF)$_2$PF$_6$ single crystals was measured along all three directions, a, b', and c^*. Deviations of the microwave response from the dc activation energy indicate that the pinned mode resonance is present in the a and b' axes response, but not along the least conducting c^* direction. The behavior can be explained by the nesting properties of the quasi one-dimensional conductor.

In addition, the electric-field dependence of the collective transport was studied in the radiofrequency and microwave range. The SDW response is non-linear above an ac threshold field because the SDW is driven into metastable states with longer relaxation times; this threshold is strongly reduced at temperatures below 4 K. In the non-linear regime, radio-frequency dielectric measurements have identified, for the first time, two length and time scales involved in the low-temperature dynamics of the spin-density-wave state of $(TMTSF)_2PF_6$. In addition to the well known screened phason relaxation with Arrhenius-like decay determined by single-particle gap, there is an additional mode at lower frequencies with a temperature-independent relaxation time found at temperatures between 4 K and 2 K. We ascribe this mode to discommensurations, that is, to short-wavelength excitations of the SDW close to commensurability. With increasing ac field, the screened phason loss-peak and the pinned-mode resonance shift to lower frequencies due to increasing contributions of long-time processes. From our microwave experiments we conclude that this behavior occurs in the a and b' directions. Finally, below $T = 1.7$ K, only one screened phason-like loss-peak can be detected whose relaxation is governed by low energy barriers of about half single-particle gap. How this relaxation mode further evolves with decreasing temperature, and if discommensurations disappear completely from the picture, should be clarified by further work.

We thank Gabriele Untereiner for the crystal growth and sample preparation. The work was supported by the Deutsche Forschungsgemeinschaft (DFG) and Croatian Ministry of Science.

References

1. D. Jérome, H.J. Schulz, Adv. Phys. **31**, 299 (1982)
2. G. Grüner, Rev. Mod. Phys. **66**, 1 (1994)
3. G. Grüner, *Density Waves in Solids* (Addison-Wesley, Reading, 1994)
4. T. Takahashi, Y. Maniwa, H. Kawamura, G. Saito, J. Phys. Soc. Jpn. **55**, 1364 (1986)
5. L. Degiorgi, M. Dressel, A. Schwartz, B. Alavi, G. Grüner, Phys. Rev. Lett. **76**, 3838 (1996); M. Dressel, L. Degiorgi, J. Brinkmann, A. Schwartz, G. Grüner, Physica B **230-232**, 1008 (1997); V. Vescoli, L. Degiorgi, M. Dressel, A. Schwartz, W. Henderson, B. Alavi, G. Grüner, J. Brinkmann, A. Virosztek, Phys. Rev. B **60**, 8019 (1999)
6. G. Mihály, A. Virosztek, G. Grüner, Phys. Rev. B **55**, 13456 (1997)
7. S. Donovan, M. Dressel, Y. Kim, L. Degiorgi, G. Grüner, W. Wonneberger, Phys. Rev. B **49**, 3363 (1994)
8. S. Tomić, J.R. Cooper, D. Jérome, K. Bechgaard, Phys. Rev. Lett.**62**, 462 (1989); W. Kang, S. Tomić, D. Jérome, Phys. Rev. B **43**, 1264 (1991); S. Tomić, J.R. Cooper, W. Kang, D. Jérome, K. Maki, J. Phys. I France **1**, 1603 (1991)
9. G. Mihály, Y. Kim, G. Grüner, Phys. Rev. Lett. **67**, 2713 (1991); G. Mihály, Y. Kim, G. Grüner, Phys. Rev. Lett. **66**, 2806 (1991); O. Trætteberg, G. Kriza, G. Mihály, Phys. Rev. B **45**, 8795 (1992); F. Zámborszky, G. Szeghy, G. Abdussalam, G. Mihály, Phys. Rev. B **60**, 4414 (1999)
10. K. Nomura, T. Shimizu, K. Ichimura, T. Sambongi, M. Tokumoto, H. Anzai, N. Kigoshita, Solid State Commun. **72**, 1123 (1989); M. Basletić, N. Biškup, B. Korin-Hamzić, A. Hamzić, S. Tomić, Fizika A **8**, 293 (2000)
11. G. Kriza, G. Quirion, O. Trætteberg, W. Kang, D. Jérome, Phys. Rev. Lett. **66**, 1922 (1991)
12. W.G. Clark, M.E. Hanson, W.H. Wong, B. Alavi, J. Phys. IV France **3**, C2-235 (1993); W.G. Clark, M.E. Hanson, W.H. Wong, B. Alavi, Physica B **194-196**, 285 (1994); W.H. Wong, M.E. Hanson, B. Alavi, W.G. Clark, W.A. Hines, Phys. Rev. Lett. **70**, 1882 (1993); W.H. Wong, M.E. Hanson, W.G. Clark, B. Alavi, G. Grüner, Phys. Rev. Lett. **72**, 2640 (1994)
13. T. Takahashi, Y. Maniwa, H. Kawamura, K. Murata, G. Saito, Synth. Met. **19**, 225 (1987); T. Takahashi, T. Harada, Y. Kobayashi, K. Kanoda, K. Suzuki, K. Murata, G. Saito, Synth. Met. **41**, 3985 (1991)
14. J. Odin, J.C. Lasjaunias, K. Biljaković, P. Monceau, K. Bechgaard, Solid State Comm. **91**, 523 (1994)
15. M. Basletic, B. Korin-Hamzic, K. Maki, Phys. Rev. B **65**, 235117 (2002)
16. M. Dressel, K. Petukhov, B. Salameh, P. Zornoza, T. Giamarchi, Phys. Rev. B **71**, 075104 (2005)
17. M. Pinterić, T. Vuletić, S. Tomić, J.U. von Schütz, Eur. Phys. J. B **22**, 335 (2001)
18. O. Klein, S. Donovan, M. Dressel, G. Grüner, Int. J. Infrared and Millimeter Waves **14**, 2423 (1993); S. Donovan, M. Dressel, O. Klein, K. Holczer, G. Grüner, Int. J. Infrared and Millimeter Waves, **14**, 2459 (1993); M. Dressel, O. Klein, S. Donovan, G. Grüner, Int. J. Infrared and Millimeter Waves, **14**, 2489 (1993)
19. M. Dressel, G. Grüner, *Electrodynamics of Solids* (Cambridge University Press, Cambridge, 2002)
20. K. Petukhov, M. Dressel, Phys. Rev. B **71**, 073101 (2005)
21. Note, the microwave data displayed in Figure 3, 4, and 6 are taken at different samples; their absolute values of resistivity vary. For microwave experiments it is also known that the absolute values also contain a large uncertainty due to the geometry (depolarization factor) [18]
22. W.M. Walsh Jr., F. Wudl, G.A. Thomas, D. Nalewajek, J.J. Hauser, P.A. Lee, T. Poehler, Phys. Rev. Lett. **45**, 829 (1980)
23. A. Jànossy, M. Hardiman, G. Grüner, Solid State Commun. **46**, 21 (1983)
24. L.I. Buravov, V.N. Laukhin, A.G. Khomenko, Sov. Phys. JETP **61**, 1292 (1985)
25. H.H.S. Javadi, S. Sridhar, G. Grüner, L. Chiang, F. Wudl, Phys. Rev. Lett. **55**, 1216 (1985)
26. The only exception is the 3 GHz measurement, which was performed in a split ring resonator and not a enclosed cavity
27. T. Vuletić, D. Hermna, N. Biškup, M. Pinterić, A. Omerzu, S. Tomić, M. Nasagawa, J. Phys. IV France **9**, PR10-275 (1999)
28. R.J. Cava, R.M. Flemming, R.G. Dunn, E.A. Rietman, L.F. Schneemeyer, Phys. Rev. B **30**, 7290 (1984)
29. M. Pinterić, M. Miljak, N. Biškup, O. Milat, I. Aviani, S. Tomić, D. Schweitzer, W. Strunz, I. Heinen, Eur. Phys. J. B **11**, 217 (1999)
30. W.L. McMillan, Phys. Rev. B **14**, 1496 (1976)
31. M. Pinterić, T. Vuletić, M. Lončarić, S. Tomić, J.U. von Schütz, Eur. Phys. J. B **16**, 487 (2001); S. Tomić, M. Pinterić, T. Vuletić, J.U. von Schütz, D. Schweitzer, Synth. Met. **120**, 695 (2001)